

Validity of simplified Shockley-Read-Hall statistics for modeling carrier lifetimes in crystalline silicon

Daniel Macdonald* and Andrés Cuevas

Department of Engineering, FEIT, The Australian National University, Acton ACT, 0200, Australia

(Received 11 February 2002; revised manuscript received 15 May 2002; published 7 February 2003)

The Shockley-Read-Hall model, in its simplest and most common form, is often used to describe both injection- and temperature-dependent carrier lifetime measurements. Such lifetime modeling has provided the basis for ultrasensitive spectroscopic techniques for the study of recombination centers in crystalline silicon. However, this approximate model is only valid when the density of recombination centers is small enough to avoid trapping effects, which cause distortions in the excess mobile carrier concentrations. In this work, the simplified Shockley-Read-Hall model is compared with a more general solution of the continuity equations that takes account of carrier trapping. This comparison leads to an expression for the upper limit on the recombination center density for which the simplified Shockley-Read-Hall model remains accurate. The limit depends not only on the dopant density, but also on the energy level and electron and hole capture cross sections for a given type of recombination center. The results allow experimental conditions that do not invalidate the use of the simplified Shockley-Read-Hall model to be determined.

DOI: 10.1103/PhysRevB.67.075203

PACS number(s): 72.20.Jv, 71.55.Cn

I. INTRODUCTION

Techniques based on carrier lifetime measurements have been developed recently with the common goal of characterizing impurities in crystalline silicon. One approach, which has been referred to as injection-dependent lifetime spectroscopy (IDLS),¹ involves fitting Shockley-Read-Hall theory to injection-level-dependent lifetime measurements. Within certain constraints, such a procedure allows the energy level and carrier capture cross sections of an impurity to be determined, often with superior sensitivity and accuracy to conventional techniques such as deep-level transient spectroscopy. The IDLS technique has recently been applied to boron-oxygen complexes in Czochralski silicon^{2,3} and also to iron-boron pairs in silicon,⁴⁻⁶ as well as other metallic species such as chromium, molybdenum, and titanium.^{7,8} Previously, it had been employed in analysis of recombination centers at silicon dioxide/silicon⁹ and silicon nitride/silicon interfaces,^{9,10} which are of critical importance in solar cell applications. It has also been used to characterize recombination centers in electron-irradiated silicon.^{11,12} In fact, simplified variations of the technique effectively formed the basis of well-known, pioneering studies of iron-boron¹³ and chromium-boron¹⁴ pairs in silicon.

A second group of lifetime-based techniques, recently dubbed temperature-dependent lifetime spectroscopy (TDLS), has also been developed.¹ By analyzing the temperature dependence of the low-injection lifetime, the energy level of the dominant recombination centers can be inferred. So far it has found application in analysis of iron-related centers¹⁵⁻¹⁷ and various other metallic centers,¹⁸ as well as electron-irradiated silicon.^{11,12} It appears certain that lifetime-based techniques such as IDLS and TDLS will become more widespread as increasingly sensitive techniques are needed to track ever-diminishing quantities of impurities, and as the requirements of electronic devices become ever more stringent.

These two techniques rely heavily on the use of Shockley-Read-Hall^{19,20} (SRH) statistics to model the behavior of the recombination lifetime as a function of either injection level or temperature. However, they generally make use of a simplified version of SRH theory that involves a number of assumptions^{21,22} that must be satisfied when applying the model to experimental data. The most restrictive of these requires almost equal excess “untrapped” electron and hole concentrations. As the recombination center density N approaches a critical value N_{crit} , this simplified SRH model becomes increasingly inaccurate, due to the fact that the recombination centers in general also act as “traps.” When this occurs, carriers spend some finite time trapped at the center before either recombining or being ejected back into the band from which they came. Such trapping alters the overall carrier dynamics, often very significantly, and even if only one type of carrier is trapped. This restriction on the SRH model is often expressed as simply requiring that N be “small.”

The purpose of this paper is to determine exactly how small N must be to ensure the simplified SRH model remains accurate, therefore enabling lifetime-based spectroscopic techniques to be safely employed. This is achieved by comparing it with a more general model that explicitly accounts for the trapping properties of the defects and hence is valid for any value of N , provided that steady-state conditions prevail. This general model is used to find an expression for N_{crit} in terms of the dopant and excess carrier densities, and also the energy level and capture cross sections of a given recombination center. These latter parameters turn out to have significant impact on the range of validity of the simplified SRH theory. First, however, we begin with the continuity equations that provide a general description of carrier dynamics within a semiconductor, and which underpin all the recombination models considered.

II. RECOMBINATION MODELS

In a nondegenerate semiconductor under the influence of external illumination, the excess concentrations of free, un-

trapped electrons Δn and holes Δp are described by the following continuity equations:²

$$g_E - \frac{d\Delta n}{dt} = \frac{\Delta n}{\tau_n} = \frac{1}{\tau_{n0}} \left[\frac{(n_0 + n_1 + \Delta n)(\Delta n - \Delta p)}{N} + \frac{\Delta n n_1}{n_0 + n_1} \right], \quad (1)$$

$$g_E - \frac{d\Delta p}{dt} = \frac{\Delta p}{\tau_p} = \frac{1}{\tau_{p0}} \left[\frac{(p_0 + p_1 + \Delta p)(\Delta p - \Delta n)}{N} + \frac{\Delta p p_1}{p_0 + p_1} \right]. \quad (2)$$

Here, g_E is the rate of electron-hole pair generation by the illumination, n_0 and p_0 are the electron and hole concentrations in thermal equilibrium, τ_n and τ_p are the electron and hole lifetimes, and N is the recombination center density. The capture time constants for electrons and holes, τ_{n0} and τ_{p0} , are related to the capture cross sections σ_n and σ_p of the recombination center, and also to the recombination center density and the thermal velocities of electrons and holes v_{th} , via the following expressions:

$$\tau_{n0} = \frac{1}{N\sigma_n v_{th}}, \quad \tau_{p0} = \frac{1}{N\sigma_p v_{th}}. \quad (3)$$

The assumption of nondegeneracy is required to provide an unambiguous meaning to the capture cross sections, since they represent ‘‘average’’ cross sections for carrier capture from *all* possible band states.²¹ The statistical factors n_1 and p_1 are the equilibrium concentrations of electrons and holes, respectively, when the Fermi level coincides with the energy of the recombination center E_T :

$$n_1 = N_C \exp\left(\frac{E_T - E_C}{kT}\right), \quad p_1 = N_V \exp\left(\frac{E_C - E_G - E_T}{kT}\right), \quad (4)$$

where E_C is the conduction-band-edge energy and E_G the energy gap. The densities of states at the conduction- and valence-band edges N_C and N_V are $N_C = 2.86 \times 10^{19}$ and $N_V = 3.10 \times 10^{19} \text{ cm}^{-3}$ for silicon at room temperature.²³

The continuity Eqs. (1) and (2) allow for all the possible interactions between the bands and the recombination centers, namely recombination via capture of an electron (or hole) and subsequent capture of a hole (or electron), or trapping via capture and release of an electron (or hole). The tendency of a specific recombination center to act primarily

as a trap or a recombination site, or as some combination of both, will depend on its energy and capture cross sections, and also on the Fermi level.

As discussed by Blakemore,²¹ the time-dependent continuity Eqs. (1) and (2) can only be solved analytically under very special conditions, which are not of great practical interest. In the general case, complications arise due to the coupled nature of these expressions, which is a direct consequence of the fact that the centers may act as both recombination sites and as traps. Under steady-state conditions, however, the time-dependent terms are zero, the equations are less strongly coupled, and general solutions do exist. This was exploited by Shockley and Read,¹⁹ whose Eq. (4.4) is precisely such a solution, the only underlying assumptions being those of nondegeneracy and steady-state conditions. Cast in this form, SRH theory is indeed quite general. However, in subsequent sections of their paper, Shockley and Read went on to develop only cases with restricted application. The first of these, in their Secs. V and VI, was for arbitrary modulation (values of Δn and Δp) but only small values of N . A later case, in Appendix A, was for arbitrary N but only small modulation. It is the first of these restricted manifestations of SRH theory, i.e., for small N , which is most widely used today. We shall refer to it as the ‘‘simplified’’ SRH model, following the heading of Shockley and Read’s own Sec. V.

One route to the simplified SRH expression from the continuity equations involves eliminating N by substitution from Eqs. (1) into (2) under steady-state conditions. After some rearranging, and upon use of the identities $n_0/(n_0 + n_1) = p_1/(p_0 + p_1)$ and $p_1 n_1 = p_0 n_0$, the result is

$$g_E = \frac{\Delta n}{\tau_n} = \frac{\Delta p}{\tau_p} = \frac{p_0 \Delta n + n_0 \Delta p + \Delta n \Delta p}{\tau_{p0}(n_0 + n_1 + \Delta n) + \tau_{n0}(p_0 + p_1 + \Delta p)}. \quad (5)$$

Further manipulation of this expression, along with the assumption of vanishing excess carrier densities, leads to Eq. (A7) of Shockley and Read, which is the case for arbitrary N but restricted to small modulation. If, on the other hand, arbitrary excess carrier densities are allowed, but we insist that N is small enough to not noticeably perturb them, so that $\Delta n = \Delta p$, then we are led directly to Eq. (5.3) from Shockley and Read, the simplified SRH model:

$$\tau_{\text{SRH}} = \tau_n = \tau_p = \frac{\tau_{p0}(n_0 + n_1 + \Delta n) + \tau_{n0}(p_0 + p_1 + \Delta n)}{n_0 + p_0 + \Delta n}. \quad (6)$$

Note that the simplifying assumption merely requires that $\Delta n = \Delta p$, but it is not clear exactly how small N must be to ensure this is so. This generates some uncertainty in applying the simplified SRH model to experimental data. As mentioned, however, this expression is widely employed in modeling carrier recombination for applications such as IDLS and TDLS. In order to quantify the limitations of the SRH model, it is useful to compare it with a more general solution to the continuity equations.

Blakemore has shown that general solutions of the continuity equations can be relatively easily found for the case of arbitrary excess carrier densities and values of N , making the assumptions in the simplified SRH model largely unnecessary. The only disadvantage of these general solutions over the simplified SRH model is that they are long.

When steady-state conditions prevail, the continuity Eqs. (1) and (2) may be written as

$$g_E = \frac{1}{\tau_{n0}} \left[\frac{(n_0 + n_1 + \Delta n)(\Delta n - \Delta p)}{N} + \frac{\Delta n n_1}{n_0 + n_1} \right] \\ = \frac{1}{\tau_{p0}} \left[\frac{(p_0 + p_1 + \Delta p)(\Delta p - \Delta n)}{N} + \frac{\Delta p p_1}{p_0 + p_1} \right]. \quad (7)$$

This expression represents two equations containing three unknowns: Δn , Δp , and g_E . Manipulating the two expressions on the right-hand side of Eq. (7) gives a quadratic equation involving only Δn and Δp . Upon applying the identities $n_0/(n_0 + n_1) = p_1/(p_0 + p_1)$ and $p_1 n_1 = p_0 n_0$, the solution may be written as²¹

$$\Delta n = \sqrt{\frac{1}{4} [A + \Delta p(k+1)]^2 - \Delta p N \left(\frac{p_0 - k p_1}{p_0 + p_1} \right)} \\ - \frac{1}{2} [A + \Delta p(k-1)], \quad (8)$$

where we have defined $k = \tau_{n0}/\tau_{p0}$ and

$$A = \frac{N p_0}{p_0 + p_1} + k(p_0 + p_1) + n_0 + n_1. \quad (9)$$

By choosing a range of values for Δp , we may calculate the corresponding values first for Δn , then g_E , and finally the carrier lifetimes via $\tau_n = \Delta n/g_E$ and $\tau_p = \Delta p/g_E$. The injection-level-dependent lifetime curves obtained in this way may then be compared with the simplified SRH model. Of course it is also possible to express τ_n directly in terms of Δn and N , similarly for τ_p in terms of Δp and N . As expected, these expressions reduce to the familiar simplified SRH model when N is small. However, they are lengthy both to derive and express, as illustrated by Blakemore²¹ in his Sec. 8.4, while the more compact approach shown here is more easily computed.

Note that if N is small then Eq. (8) simplifies to $\Delta n = \Delta p$, as expected. Under these conditions the results will be identical to the simplified SRH model. However, in the general case $\Delta n \neq \Delta p$ and, therefore, $\tau_n \neq \tau_p$. This point has recently been highlighted by Karazhanov,^{24,25} who used Eq. (5) in conjunction with the electroneutrality condition to calculate Δn and Δp and, therefore, τ_n and τ_p . In contrast, the approach used here involves direct solution of Eqs. (1) and (2), which implicitly contain the electroneutrality condition.

It may seem logical at this point to suggest replacing the use of the simplified SRH model in lifetime spectroscopy applications with this more general solution of the continuity equation. Indeed, this would entirely remove the need to be watchful for trapping effects. However, the general solution requires explicit knowledge of the value of N , while the sim-

plified SRH model does not (although even in the simplified case N is required to determine the capture cross sections, but not the capture time constants). In many practical cases the value of N is not known, and so the simplified model may be the most useful, despite the restricted range over which it is valid.

A final point to note regarding these models is that they both neglect the possibility of tunneling transitions *between* recombination centers. If the wave functions of these localized states overlap to an appreciable extent, then such tunneling transitions can affect properties such as lifetime and mobility. A well-known example is amorphous silicon, which contains band-tail states of sufficiently high concentration to allow ‘‘hopping’’ between them. Hattori *et al.*²⁶ recently developed a recombination model for amorphous silicon that contained three types of electronic states: the bands themselves, the band tails, and deep states. Their model allowed transitions between the bands and both the band-tail and deep states, as well as between the band-tail states and the deep states. They also included tunneling transitions between band-tail states, and found that these were largely responsible for the form of measured drift mobility data. They did not, however, include tunneling transitions between deep states, since their density was kept below 10^{17} cm^{-3} , and hence their wave functions are very unlikely to overlap. Similarly, in this work, we neglect tunneling transitions between the deep states, and any impact this might have on the lifetime, since in almost all practical cases the density of recombination centers will be well below 10^{17} cm^{-3} . Band tails do not normally exist in crystalline silicon, unless it is extremely heavily doped, and so we do not include their effects here either.

III. COMPARISON OF THE TWO MODELS

Figure 1 provides a direct comparison between the general steady-state solution derived above and the SRH model for the specific case of interstitial iron in crystalline silicon. This particular recombination center, which has an energy level²⁷ of $E_v + 0.38 \text{ eV}$ and capture cross sections of $\sigma_n = 5 \times 10^{-14}$ and $\sigma_p = 7 \times 10^{-17} \text{ cm}^{-2}$, was chosen because it provides a good example of the behavior of a ‘‘deep’’ center. Three different values of the iron concentration are shown on the plot. For each of these, four lifetime curves are plotted: the simplified SRH lifetime, the electron and hole lifetimes from the general steady-state solution, and a mobility-weighted combination of these electron and hole lifetimes. The latter weighted curve will most accurately reflect lifetime measurements from photoconductance-based methods, which are unable to discriminate between carrier type since they merely record changes in conductivity. The weighted lifetime is calculated via $\tau_{\text{wtd}} = \Delta p_{\text{wtd}}/g_E$, where the mobility-weighted excess carrier density Δp_{wtd} is given by

$$\Delta p_{\text{wtd}} = \frac{\Delta n \mu_n + \Delta p \mu_p}{\mu_n + \mu_p}. \quad (10)$$

The four curves that represent the lowest concentration of iron are all in good agreement. In this case, the small con-

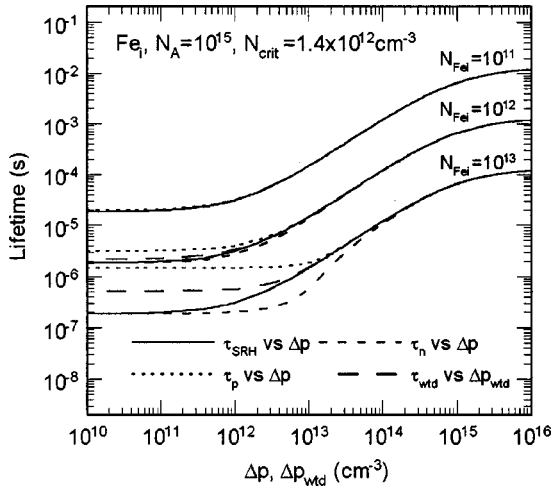


FIG. 1. Comparison between the injection-level dependence of the simplified SRH lifetime and the electron and hole lifetimes as calculated from the general steady-state solution, using the recombination parameters of interstitial iron. Curves are shown for three values of the iron concentration. The electron and hole lifetimes are plotted against the excess hole concentration Δp . Also shown for each iron concentration is a fourth curve, τ_{wtd} , which represents the mobility-weighted combination of τ_n and τ_p plotted against a similarly weighted excess carrier concentration Δp_{wtd} .

centration of centers causes negligible trapping, or, in other words, a minimal inequality between excess mobile electron and hole concentrations. The result is electron and hole lifetimes that are almost equal at all injection levels, and hence one may safely apply the simplified SRH model in this case.

As the iron concentration increases, however, the electron and hole lifetimes start to become significantly different, especially at the lower injection levels. This reflects an increasing breakdown of the simplified SRH model. The mobility-weighted lifetime curves reveal that the large hole lifetime causes the simplified SRH model to underestimate data obtained by photoconductance-based techniques. Note, however, that the curves are still in good agreement at higher injection levels.

The trends shown in Fig. 1 are characteristic of deep recombination centers, which always generate lifetimes that increase (or remain constant) with increasing injection level.¹ In contrast, shallow centers can result in either increasing or decreasing lifetimes, depending on the dopant density and the exact value of the energy level.²¹ FeB pairs provide an example of shallow centers in silicon. Figure 2 gives a comparison of the SRH model and the general steady-state solution for FeB pairs, with an energy level²⁷ of $E_C - 0.23$ eV and capture cross sections⁶ of $\sigma_n = 3 \times 10^{-14}$ and $\sigma_p = 2 \times 10^{-15}$ cm². Once again, the results show that the SRH theory becomes increasingly inaccurate as the recombination center density increases. For modern spectroscopy techniques that rely on the use of SRH theory, the important question then becomes, what is the critical recombination center density above which the simplified SRH model will be inaccurate? This question is addressed in the following section.

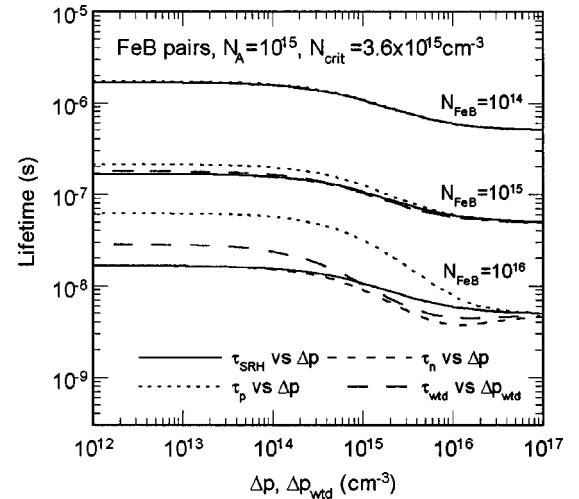


FIG. 2. Comparison between the injection-level dependence of the simplified SRH lifetime and the electron and hole lifetimes as calculated from the general steady-state solution, using the recombination parameters of FeB pairs.

IV. THE CRITICAL RECOMBINATION CENTER DENSITY

The upper limit on the recombination center density N for which the simplified model is accurate will depend on the particular properties of the recombination center (i.e., the energy level and capture cross sections), and also on the dopant density. In general, it will also depend on the concentration of excess carriers, since, if sufficiently numerous, these may overwhelm any trapping effects. A convenient way to express this limit is by defining a parameter N_{crit} , such that the simplified SRH model is only valid if $N \ll N_{\text{crit}}$.

A direct approach to calculating N_{crit} is to consider the excess carrier ratio $\Delta n/\Delta p$ as determined by the general steady-state model above. For conditions under which the simple SRH model is accurate, trapping must be negligible, and this ratio will be close to unity. An expression for $\Delta n/\Delta p$ can be arrived at from Eq. (7):

$$\frac{\Delta n}{\Delta p} = \frac{n_0 + n_1 + \Delta n + k(p_0 + p_1 + \Delta p) + kp_1 N / (p_0 + p_1)}{n_0 + n_1 + \Delta n + k(p_0 + p_1 + \Delta p) + p_0 N / (p_0 + p_1)}. \quad (11)$$

First, it is clear from this expression that the right-hand side will always equal unity when

$$p_0 = kp_1 = \frac{\tau_{n0}}{\tau_{p0}} p_1. \quad (12)$$

If this condition holds, trapping will *always* be negligible, irrespective of the recombination center density N . In practice, however, this condition is only satisfied by rare coincidence. In physical terms, it represents the unique combination of energy level and capture cross sections that cause a perfect balance between majority- and minority-carrier trapping.²¹

In the more general case, the right-hand side of Eq. (11) will also be close to unity when the two terms involving N either do not contribute much to the numerator or denominator, or contribute very similarly. A convenient way to express this in a single inequality is to state that the *magnitude of their difference* must be much less than the other terms. After some rearranging, we then arrive at the following expression for N_{crit} .

$$N_{\text{crit}} = \frac{(p_0 + p_1)[n_0 + n_1 + \Delta n + k(p_0 + p_1 + \Delta p)]}{|p_0 - kp_1|}. \quad (13)$$

If we require the simplified SRH model to be accurate to within 10%, then N must be at least an order-of-magnitude smaller than N_{crit} . Under high-injection conditions, a greater concentration of recombination centers can be tolerated, since N_{crit} increases due to the Δn and Δp terms. However, it is often the value of N_{crit} under low-injection conditions that is of interest. For a p -type sample with $p_0 = N_A$ such that $n_0 = n_i^2/p_0$ is negligible, the relevant expression for N_{crit} in low injection is

$$N_{\text{crit}} = \frac{(N_A + p_1)(n_1 + kN_A + kp_1)}{|N_A - kp_1|}. \quad (14)$$

This expression can be simplified further if the recombination centers are deep, meaning that both p_1 and $n_1 \ll N_A$. In such cases, provided k is not excessively large, then

$$N_{\text{crit}} = N_A \frac{\tau_{n0}}{\tau_{p0}}. \quad (15)$$

This final expression in fact represents the lowest possible, and hence most restrictive, value for N_{crit} for *any* recombination center energy, deep or shallow. In this sense, deep levels are most likely to cause the simplified model to become invalid for a given value of N . This does not necessarily mean, however, that they will always be the most difficult to study using the simplified SRH model. In general, fewer deep recombination centers are required to produce a given lifetime, counterbalancing the fact that N_{crit} is smaller for such centers.

Another important feature of this final expression is that N_{crit} depends only on the *ratio* of τ_{n0} and τ_{p0} , and not on their magnitudes. This reflects the fact that the centers must not cause significant trapping of carriers, as has been discussed above. The extent to which this trapping occurs is characterized by the ratio τ_{n0}/τ_{p0} , since this is essentially a measure of the proportion of time that the carriers remain untrapped. It is not surprising then that this parameter has a heavy bearing on the boundaries of accuracy of the simple SRH model.

It is worth noting at this point that Shockley and Read also considered under which conditions their simplified theory would be valid (as discussed in their Appendix A). They concluded that the simplification would hold provided N is small compared with any one of n_0 , p_0 , n_1 , or p_1 . However, the conditions under which they arrived at this conclusion were only valid for infinitesimal modulation. In

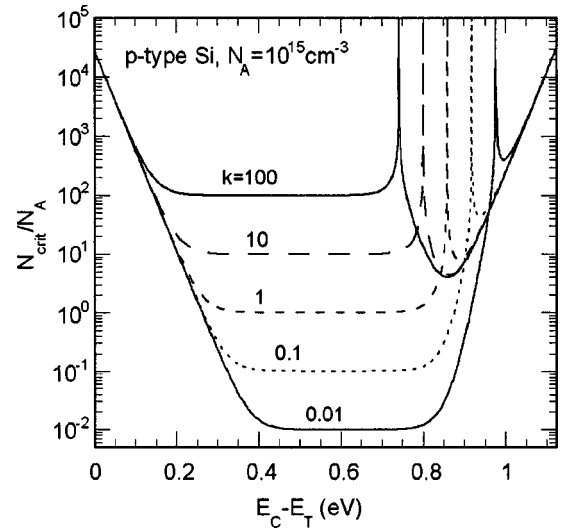


FIG. 3. Values of the low-injection limit of N_{crit} , normalized with respect to $N_A = 10^{15} \text{ cm}^{-3}$, as a function of the recombination center energy level $E_C - E_T$. Curves are shown for different values of the capture cross-section ratio k .

contrast, the expression for N_{crit} given in this work also accounts for arbitrary modulation, hence the appearance of Δn . Furthermore, the expression derived here also accounts for the potential impact of highly asymmetric cross sections, as manifested in the value of k , which was not considered in Shockley and Read's approximate approach.

Figure 3 depicts the dependence of the low-injection limit of N_{crit} , normalized with respect to N_A , as a function of the recombination center energy, which appears indirectly in Eq. (14) through n_1 and p_1 . Five curves are shown, corresponding to different values of the capture cross-section ratio k . The spikes on the curves correspond to the conditions of Eq. (12)—a very special and narrow range of energies for which the effect of trapping will be negligible. Of more general interest, however, is the fact that the curves show that there is a broad range of energy levels near the middle of the band gap that has the most detrimental impact on N_{crit} . These are referred to as deep centers, and the magnitude of their impact on N_{crit} is determined directly by the value of k .

Figure 4 shows that the breadth of the flat region due to deep centers is determined by the dopant density. For lightly doped samples, the range of recombination energies that generates the most severe trapping is reduced. Furthermore, shallow centers of a given energy level impose a less stringent limit on N_{crit} in more lightly doped material. Figures 3 and 4 reveal that whether a center behaves as a deep center or not depends not only on its energy, but also on the dopant density and the value of k . Therefore, care must be taken to avoid applying Eq. (15) to centers that, despite having energy levels far from the band edges, may not behave as deep states. It should be noted that in both Figs. 3 and 4, the value of N_{crit} exceeds 10^{17} cm^{-3} at some points. It is possible that tunneling transitions between the deep states would significantly alter the carrier dynamics if the actual value of recombination centers N also exceeded this value. In such cases a more complex model such as that developed by Hattori *et al.* would be required.

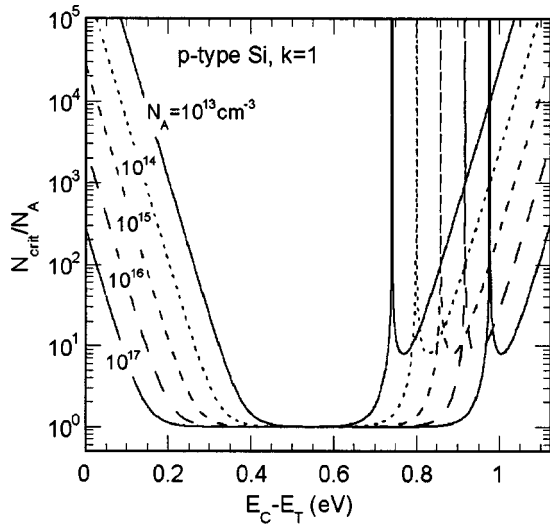


FIG. 4. Values of the low-injection limit of N_{crit} , normalized with respect to N_A , as a function of the recombination center energy level $E_C - E_T$. Curves are shown for different values of N_A . The capture cross-section ratio k is unity.

If a recombination center is known to be deep, then N_{crit} is given by Eq. (15) for low-injection conditions. As discussed above, interstitial iron is a deep center in silicon, and its low value of k results in a limit of $N_{\text{crit}} = 1.4 \times 10^{12} \text{ cm}^{-3}$ for the dopant density in Fig. 1 ($N_A = 10^{15} \text{ cm}^{-3}$). The plots in Fig. 1 show that when $N \ll N_{\text{crit}}$ (i.e., the $N = 10^{11} \text{ cm}^{-3}$ case), the SRH model is accurate across all injection levels. For higher recombination center densities, mid- to high-injection lifetime measurements may still be accurately modeled with SRH theory, provided the excess carrier concentration is high enough to ensure that $N \ll N_{\text{crit}}$, where N_{crit} is given by Eq. (13).

For shallow centers, the value of N_{crit} depends on the factors n_1 and p_1 also. An example of such a shallow center is given by FeB pairs, which give a value of $N_{\text{crit}} = 3.6 \times 10^{15} \text{ cm}^{-3}$ for the conditions in Fig. 2 ($N_A = 10^{15} \text{ cm}^{-3}$). Once again, the curves reveal that the value of N_{crit} provides an effective demarcation between the regions over which SRH theory is valid for all injection levels and those over which it is not. It should be noted that, while referred to as shallow, FeB pairs are still some considerable distance from the conduction-band edge. As a result, the terms containing n_1 and p_1 in Eq. (13) moderate the value of N_{crit} , but not to a massive extent. However, for very shallow centers, N_{crit} is likely to be much larger, due to the overwhelming magnitude of either p_1 or n_1 .

A. Modeling more than one type of center simultaneously

In many practical situations, more than one type of recombination center may be present in significant quantities. As mentioned, one such example is provided by interstitial iron and FeB pairs. Both centers may occur with similar concentrations, and both may impact significantly on the overall, or *effective*, recombination lifetime.

A question naturally arises as to how to correctly deal with such cases. A common approach is to treat the different

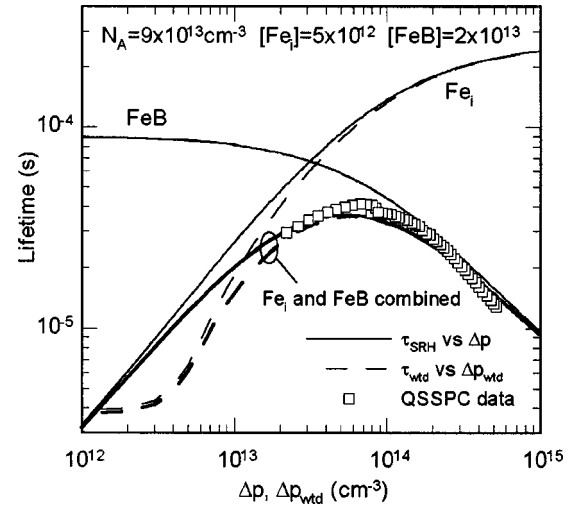


FIG. 5. Comparison between experimental data (from Ref. 6) and modeled lifetime curves for a silicon sample containing interstitial Fe and FeB pairs as the dominant recombination sources.

types of recombination centers as “independent,” and then proceed to sum the inverse lifetimes due to each type of center to obtain the effective lifetime.

In using this approach, it is assumed that any additional terms arising from interactions between the various types of centers are negligible.²¹ If being used in conjunction with the simplified SRH model, it is only valid when *all* types of recombination centers are present in small enough quantities to avoid trapping, that is, they must all satisfy the requirement $N \ll N_{\text{crit}}$. Even if only one such center traps carriers to any significant extent, the resulting change in the free-carrier populations can cause very large changes to the recombination dynamics of *all* the centers. An extreme case is described by the Hornbeck-Haynes model,²⁸ which was developed for the situation in which one type of center acts only as a recombination center, and another only as a trap. This model shows that the trapping centers do indeed have a dramatic impact on the behavior of the recombination centers, and has been used to explain unusual photoconductance measurements in single-crystal silicon and germanium^{28–30} and multicrystalline silicon.³¹

B. An experimental example

Figure 5 shows photoconductance-based lifetime measurements, taken from Ref. 6, of a silicon sample with a total Fe concentration of $2.5 \times 10^{13} \text{ cm}^{-3}$. The iron was introduced by ion implantation, and the sample annealed to distribute the iron uniformly throughout the bulk, taking care to avoid precipitation.⁶ The lifetime measurement was performed using the quasi-steady-state photoconductance technique.³² Unfortunately, it was not possible to measure the iron-related lifetime at lower carrier densities than shown, because of the existence of trapping centers associated with the surface passivating film, which overwhelm the photoconductance.⁶ In this sample, only 20% of the iron was present in interstitial form, and the rest was paired with boron dopant ions.

Also shown are the simplified SRH lifetimes for the relevant concentrations of Fe_i and FeB pairs, calculated using the capture cross sections and energy levels given above, as well as the combined lifetime achieved by adding the inverses of these two components. The general, mobility-weighted steady-state solutions are also shown. The general solution and the simplified model are in good agreement for all injection levels for the FeB pairs, but a discrepancy emerges at lower carrier concentration for Fe_i . As a result, a similar disagreement appears for the combined recombination lifetimes.

The values of N_{crit} for this dopant density ($9 \times 10^{13} \text{ cm}^{-3}$) are 1.6×10^{11} and $3.6 \times 10^{15} \text{ cm}^{-3}$ for interstitial iron and FeB pairs, respectively. Therefore, we expect the simplified theory to be valid for all injection levels for the FeB pair component, since $N_{\text{FeB}} \ll N_{\text{crit-FeB}}$. This is clearly not true for the interstitial iron component, however. As a result, the simple SRH model is not valid for this sample across all injection levels. However, at higher injection levels the simplified model remains valid due to the swamping of the trapping effects by excess carriers. For trapping effects to impact on the measurement by no more than 10%, we require that $N_{\text{crit-Fe}_i}$ be an order-of-magnitude larger than $N_{\text{Fe}_i} = 5 \times 10^{12} \text{ cm}^{-3}$. From Eq. (13), this is satisfied when $\Delta n = \Delta p = 4.5 \times 10^{13} \text{ cm}^{-3}$. Figure 5 shows that this is indeed the region in which the general model and the simplified SRH model converge within 10% for the Fe_i curves.

Since interstitial iron accounts for about only half of the total recombination lifetime at this carrier density, the effective value for Δp is around $2 \times 10^{13} \text{ cm}^{-3}$.

V. CONCLUSIONS

The simplified Shockley-Read-Hall model is a powerful and widely used tool in lifetime-based techniques for characterizing impurities and defects in semiconductors. However, to be confident that its use is valid, it is necessary to verify that the recombination center density N is small enough to avoid excessive trapping effects. An expression for the critical value of N , above which the simplified SRH model becomes invalid, has been presented. It reveals that the most severe restrictions on the region of validity of the simplified SRH model occur for deep centers with highly asymmetric capture cross sections. These restrictions should be considered routinely when using spectroscopic techniques based on either injection-level or temperature-dependent lifetime modeling.

ACKNOWLEDGMENTS

This work has been supported by the Australian Research Council. The authors wish to acknowledge the assistance of J. Wong-Leung, H. Tan, and C. Jagadish of the Research School of Physical Sciences and Engineering, ANU, for assistance with sample preparation.

*Email address: daniel@faceng.anu.edu.au

- ¹S. Rein, T. Rehr, W. Warta, and S. W. Glunz, *J. Appl. Phys.* **91**, 2059 (2002).
- ²J. Schmidt, C. Berge, and A. G. Aberle, *Appl. Phys. Lett.* **73**, 2167 (1998).
- ³J. Schmidt and A. Cuevas, *J. Appl. Phys.* **86**, 3175 (1999).
- ⁴D. Walz, J.-P. Poly, and G. Kamarinos, *Appl. Phys. A: Mater. Sci. Process.* **62**, 345 (1996).
- ⁵R. Falster and G. Barionetti, in *Recombination Lifetime Measurements in Silicon, ASTM STP 1340*, edited by D. C. Gupta, F. R. Bacher, and W. M. Hughes (American Society for Testing Materials, Philadelphia, 1998), p. 226.
- ⁶D. Macdonald, A. Cuevas, and J. Wong-Leung, *J. Appl. Phys.* **89**, 7932 (2001).
- ⁷M. L. Polignano, E. Ballandi, D. Lodi, F. Pipia, A. Sabbadini, F. Zanderigo, G. Queirolo, and F. Priolo, *Mater. Sci. Eng., B* **B55**, 21 (1998).
- ⁸P. Eichinger, in *Recombination Lifetime Measurements in Silicon, ASTM STP 1340* (Ref. 5), p. 101.
- ⁹A. G. Aberle, *Crystalline Silicon Solar Cells: Advanced Surface Passivation and Analysis* (Centre for Photovoltaic Engineering, University of New South Wales, Sydney, Australia, 1999).
- ¹⁰J. R. Elmiger, R. Schieck, and M. Kunst, *J. Vac. Sci. Technol. A* **15**, 2418 (1997).
- ¹¹H. Bleichner, P. Jonsson, N. Keskitalo, and E. Nordlander, *J. Appl. Phys.* **79**, 9142 (1996).
- ¹²N. Keskitalo, P. Jonsson, K. Nordgren, H. Bleichner, and E. Nordlander, *J. Appl. Phys.* **83**, 4206 (1998).
- ¹³G. Zoth and W. Bergholz, *J. Appl. Phys.* **67**, 6764 (1990).
- ¹⁴K. Mishra, *Appl. Phys. Lett.* **68**, 3281 (1996).
- ¹⁵Y. Hayamizu, T. Hamaguchi, S. Ushio, and T. Abe, *J. Appl. Phys.* **69**, 3077 (1991).
- ¹⁶A. Kaniava, E. Gaubas, J. Vaitkus, J. Vanhellemont, and A. L. P. Rotondaro, *Mater. Sci. Technol.* **11**, 670 (1995).
- ¹⁷A. Kaniava, A. L. P. Rotondaro, J. Vanhellemont, U. Menczigar, and E. Gaubas, *Appl. Phys. Lett.* **67**, 3930 (1995).
- ¹⁸S. Rein, T. Rehr, J. Isenberg, W. Warta, and S. W. Glunz, in *Proceedings of the Sixteenth European Photovoltaic Solar Energy Conference, Glasgow, United Kingdom, 2000*, edited by H. Scheer, B. McNelis, W. Palz, H. A. Ossenbrink, and P. Helm (James & James Ltd., London, 2000), p. 1476.
- ¹⁹W. Shockley and W. T. Read, *Phys. Rev.* **87**, 835 (1952).
- ²⁰R. N. Hall, *Phys. Rev.* **87**, 387 (1952).
- ²¹J. S. Blakemore, *Semiconductor Statistics* (Pergamon, Oxford, 1962).
- ²²R. A. Smith, *Semiconductors* (Cambridge University, Cambridge, England, 1959).
- ²³M. A. Green, *J. Appl. Phys.* **67**, 2944 (1990).
- ²⁴S. Z. Karazhanov, *Semicond. Sci. Technol.* **16**, 276 (2001).
- ²⁵S. Z. Karazhanov, *J. Appl. Phys.* **88**, 3941 (2000).
- ²⁶K. Hattori, T. Hirao, Y. Musa, and H. Okamoto, *Phys. Rev. B* **64**, 125208 (2001).
- ²⁷A. A. Istratov, H. Hieslmair, and E. R. Weber, *Appl. Phys. A: Mater. Sci. Process.* **69**, 13 (1999).
- ²⁸J. A. Hornbeck and J. R. Haynes, *Phys. Rev.* **97**, 311 (1955).
- ²⁹J. R. Haynes and J. A. Hornbeck, *Phys. Rev.* **90**, 152 (1953).
- ³⁰J. R. Haynes and J. A. Hornbeck, *Phys. Rev.* **100**, 606 (1955).
- ³¹D. Macdonald and A. Cuevas, *Appl. Phys. Lett.* **74**, 1710 (1999).
- ³²R. A. Sinton and A. Cuevas, *Appl. Phys. Lett.* **69**, 2510 (1996).